AIAA JOURNAL
Vol. 37, No. 2, February 1999

Technical Notes

TECHNICAL NOTES are short manuscripts describing new developments or important results of a preliminary nature. These Notes cannot exceed 6 manuscript pages and 3 figures; a page of text may be substituted for a figure and vice versa. After informal review by the editors, they may be published within a few months of the date of receipt. Style requirements are the same as for regular contributions (see inside back cover).

Prediction of Developing Turbulent Pipe Flow by a Modified k-ε-γ Model

You Qin Wang* and R. W. Derksen†
University of Manitoba,
Winnipeg, Manitoba R3T 5V6, Canada

Introduction

THE existence of a sharp, intermittent interface between turbulent and nonturbulent flow regions in shear flows was discovered several decades ago. The first effort at including this behavior in a turbulence model was made by Libby[1] in 1975, and further development was contributed by Byggstoyl and Kollmann[2] in 1981. In 1992 Cho and Chung[3] proposed a new type of intermittency model called the k-ε-γ model. This k-ε-γ model, in contrast to Byggstoyl and Kollmann's intermittency model that employs conditional zone-averaged moments, is based on the conventional Reynolds-averaged moments. It is a more economical model compared with Byggstoyl and Kollmann's because it halves the number of partial differential equations that need to be solved. The k-ε-γ model was originally proposed for external flow, and so far no predictions have been made by this model for internal flows. Additionally, as this k-ε-γ model is based on the standard k-ε model, wall functions are required when modeling wall-bounded flows. The requirement of the wall functions limits this model's applicability in complex turbulent flows. In this Note we have proposed a new turbulent intermittency model that eliminates the need for wall functions by modifying Cho and Chung's k-ε-γ model, and for the first time we have assessed the capability of this kind of k-ε-γ model for predicting internal flows.

We chose the developing turbulent pipe flow as our test case because the inlet region of a smooth pipe is a highly intermittent region. Furthermore, the understanding of the intermittency character in the developing pipe flow is important for modeling more complicated internal flows such as problems involving strong curvature.

Turbulence Model

With the intermittency factor taken into account, the governing equations of our modified k-ε-γ model for the two-dimensional incompressible flow in a cylindrical coordinate system are as follows.

Turbulent kinetic energy:

$$\frac{\mathrm{D}k}{\mathrm{D}t} = \frac{\partial}{\partial x}\left(\frac{\nu_t}{\sigma_k}\frac{\partial k}{\partial x}\right) + \frac{1}{r}\frac{\partial}{\partial r}\left(\frac{r\nu_t}{\sigma_k}\frac{\partial k}{\partial r}\right) + \wp - \varepsilon - \frac{2\nu k}{y^2} \tag{1}$$

where y is the distance to the wall ($y = R - r$) and $\wp$ represents the production of k due to the shear and normal strains:

$$\wp = \nu_t\left(\frac{\partial U}{\partial r} + \frac{\partial V}{\partial x}\right)^2 - (\overline{u^2} - \overline{v^2})\frac{\partial U}{\partial x} \tag{2}$$

Dissipation rate:

$$\frac{\mathrm{D}\varepsilon}{\mathrm{D}t} = \frac{\partial}{\partial x}\left(\frac{\nu_t}{\sigma_\varepsilon}\frac{\partial \varepsilon}{\partial x}\right) + \frac{1}{r}\frac{\partial}{\partial r}\left(\frac{r\nu_t}{\sigma_\varepsilon}\frac{\partial \varepsilon}{\partial r}\right) + \frac{\varepsilon^2}{k}\left[C_{\varepsilon 1}\frac{\wp}{\varepsilon} - C_{\varepsilon 2}f_2 + C_{\varepsilon 4}\Gamma - \frac{2\nu k\, e^{-C_4 y^+}}{y^2\varepsilon}\right] \tag{3}$$

where

$$\Gamma = (k^{2.5}/\varepsilon^2)(\nabla|U|)\cdot(\nabla\gamma) \tag{4}$$

$$f_2 = 1 - \tfrac{0.4}{1.8}\, e^{-(k^2/6\nu\varepsilon)^2} \tag{5}$$

The vortex stretching invariant term χ, used in the ε equation of Cho and Chung,[3] is dropped in Eq. (3) because χ vanishes in two-dimensional flow.

Intermittency factor:

$$\frac{\mathrm{D}\gamma}{\mathrm{D}t} = \frac{\partial}{\partial x}\left[(1-\gamma)\frac{\nu_t}{\sigma_\gamma}\frac{\partial \gamma}{\partial x}\right] + \frac{1}{r}\frac{\partial}{\partial r}\left[r(1-\gamma)\frac{\nu_t}{\sigma_\gamma}\frac{\partial \gamma}{\partial r}\right] + S_\gamma \tag{6}$$

where

$$S_\gamma = C_{\gamma 1}\gamma(1-\gamma)\frac{\wp}{k} + C_{\gamma 2}\frac{k^2}{\varepsilon}\left[\left(\frac{\partial \gamma}{\partial x}\right)^2 + \left(\frac{\partial \gamma}{\partial r}\right)^2\right] - C_{\gamma 3}\gamma(1-\gamma)\frac{\varepsilon}{k}\Gamma \tag{7}$$

and eddy viscosity:

$$\nu_t = C_\mu f_\mu\left\{1 + C_{\mu\gamma}\frac{k^3}{\varepsilon^2}\gamma^{-m}(1-\gamma)\left[\left(\frac{\partial \gamma}{\partial x}\right)^2 + \left(\frac{\partial \gamma}{\partial r}\right)^2\right]\right\}\frac{k^2}{\varepsilon} \tag{8}$$

where

$$f_\mu = \left[1 - \exp\left(-C_3 y^+\right)\right] \tag{9}$$

The variable y^+ is the distance from the wall nondimensionalized by the friction velocity u_* and kinematic viscosity ν of the fluid. The model constants are

$$C_\mu = 0.09, \quad C_{\mu g} = 0.10, \quad m = 3.0, \quad C_{uv} = 0.33$$
$$\sigma_k = 1.0, \quad \sigma_\varepsilon = 1.3, \quad \sigma_\gamma = 1.0, \quad C_{\varepsilon 1} = 1.35$$
$$C_{\varepsilon 2} = 1.8, \quad C_{\varepsilon 4} = 0.1, \quad C_{\gamma 1} = 1.6, \quad C_{\gamma 2} = 0.15$$
$$C_{\gamma 3} = 0.16, \quad C_4 = 0.5, \quad C_3 = 0.0115$$

Numerical Procedure

The equations were discretized using Raithby and Torrance's[4] Approximate Exponential Differencing Scheme and solved by the well-established finite volume method. The SIMPLEC algorithm and staggered grids were used for the test case. The predictions are made for both $Re = 7.5 \times 10^4$ and 3.0×10^5. However, the grid independence is checked for $Re = 7.5 \times 10^4$ only using numerical experiments, i.e., repeating the calculation on a refined grids. The two grid systems are 120×99 and 240×198, respectively. In the radial direction each grid spacing was decreased by a fixed percentage from the pipe center to the wall ($k = 0.96$ for coarse grids and $k = 0.98$ for fine grids), whereas in the axial direction equal grid spacing was used. The root mean square of the difference between the fine and coarse grid solutions was calculated at nine downstream locations ($5.4 \le x/D \le 80.0$), and the difference was averaged along the radius. The nine values are between 0.005 and 0.011 for nondimensional velocity (U/U_b; U_b is the bulk velocity), between 0.11

Received March 20, 1998; revision received Oct. 22, 1998; accepted for publication Nov. 3, 1998.

*Ph.D. Candidate, Department of Mechanical and Industrial Engineering.
†Assistant Professor, Department of Mechanical and Industrial Engineering.

and 0.14 for nondimensional turbulent kinetic energy (k/u_*^2), and between 0.00 and 0.02 (for $x/D \geq 30.3$, all of the values are 0.00) for intermittency factor γ, respectively. Most of these values are much smaller than 3.0% of the maximum value of the corresponding variable that proves the solutions are grid independent. Each discretized governing equation was solved iteratively by the line Gauss–Seidel method until solution converged. Convergence was declared if the average of the absolute mass residuals throughout the computation domain was less than 10^{-13}.

A uniform profile was assumed for all quantities at the pipe inlet: $U = U_b$, $V = 0.0$, $k = 0.005U_b^2$, $\varepsilon = C_\mu^{3/4}k^{3/2}/0.03R$, and $\gamma = 0.001$. The pipe section was chosen to be sufficiently long so that fully developed conditions could be assumed to prevail at the outlet, i.e., $\partial\phi/\partial x = 0$, where ϕ can be any of U, V, k, ε, or γ. At the pipe axis symmetrical conditions were assumed for all quantities. At the wall no-slip and impermeability conditions were imposed for U, V, k, and ε, and the value of intermittency was set to be unity. The calculations were started with the following initial values: $U = U_b$, $V = 0$, $k = 0.005U_b^2$, $\varepsilon = C_\mu^{3/4}k^{3/2}/0.03R$, and $\gamma = 0.001$, i.e., the same uniform profiles that were assumed for inlet boundary conditions.

Computational Results and Discussion

Because of space restrictions, only predictions for $Re = 3.0 \times 10^5$ are presented. For such a high-Reynolds-number flow, we found that the fine grids (240×198) were required. The developments of the axial velocities in the downstream direction at five axial locations are shown in Fig. 1. The simulation results are compared with the predictions obtained using Chien's k-ε model[5] and the experimental data of Barbin and Jones[6] and Richman and Azad.[7] The reason we chose the predictions of Chien's k-ε model to compare to our predictions is that our model reduces to Chien's k-ε model in the fully turbulent zone (where $\gamma = 1.0$). The results show that in the fully turbulent zone the predictions obtained by the two models are almost identical, which validates our code. In the core region the overshoot ratio obtained from the k-ε-γ model is lower than that obtained from Chien's k-ε model so that it reproduced the data of Richman and Azad well. Clearly the k-ε-γ model predicts the mean velocity field as well as, if not better than, Chien's k-ε model. Overall the computed mean velocity distributions are in agreement with the experimental data. This result confirms the capability of the k-ε-γ model for predicting the internal flows.

The profiles of $\overline{uv}$ at $x/d = 10$, 30, 50, and 70 are presented together with the experimental data of Richman and Azad in Fig. 2. In the inlet region ($x/D = 10$) the prediction is in better agreement with the experimental data than that of Chien's k-ε model. At $x/d = 30$ the predicted values obtained by both models are greater than those in the fully developed region, which confirms earlier observations reported in the literature.[8] In the fully developed region, as expected, the values obtained from the two models are identical.

Finally, the γ distribution vs r/R is plotted in Fig. 3. Although no experimental data are available in the inlet region of a pipe, the variation of γ from unity at the wall to zero at the pipe center seems to be physically realistic. In the outlet region the γ values are close to unity at the pipe centerline, which shows that the flow has nearly reached a fully developed state at the outlet.

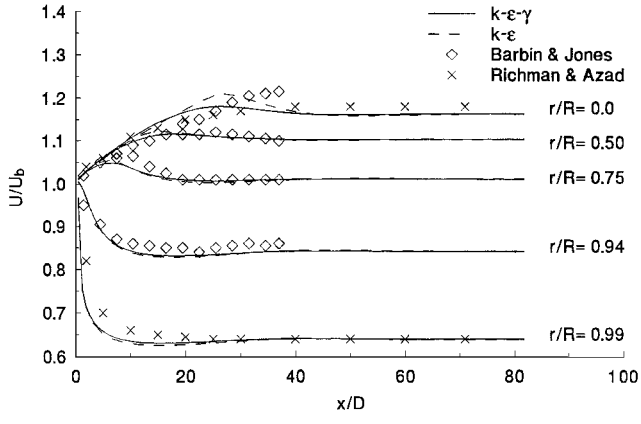

Fig. 1 Variation of axial velocity with distance downstream of pipe inlet for r/R = 0.0, 0.5, 0.75, 0.94, and 0.99 for $Re = 3.0 \times 10^5$.

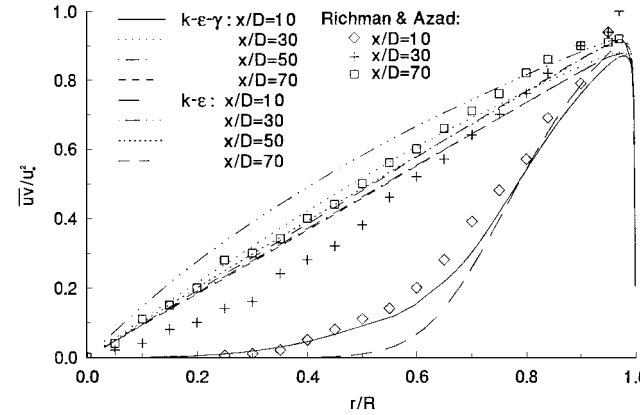

Fig. 2 Reynolds shear stress vs r/R at x/d = 10, 30, 50, and 70 for $Re = 3.0 \times 10^5$.

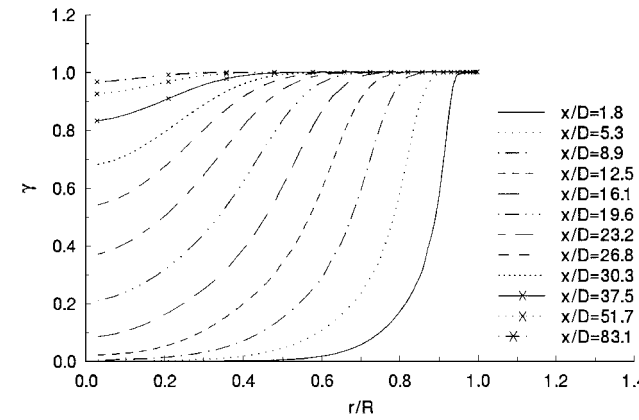

Fig. 3 Intermittency factor vs r/R at 12 different downstream positions for $Re = 3.0 \times 10^5$.

Conclusions

By modifying Cho and Chung's k-ε-γ model, a new intermittency model that eliminates the need for wall functions has been developed. This modified k-ε-γ model is capable of predicting internal flows. Furthermore, it provides better predictions for the Reynolds shear stress in the inlet region compared with predictions obtained by Chien's k-ε model.

Acknowledgments

The authors would like to acknowledge the financial support provided by the Natural Sciences and Engineering Research Council and the scholarship provided by the University of Manitoba.

References

[1] Libby, P. A., "On the Prediction of Intermittent Turbulent Flows," *Journal of Fluid Mechanics*, Vol. 68, 1975, pp. 273–295.

[2] Byggstoyl, S., and Kollmann, W., "Closure Model for Intermittent Turbulent Flows," *International Journal of Heat Mass Transfer*, Vol. 24, No. 11, 1981, pp. 1811–1822.

[3] Cho, J. R., and Chung, M. K., "A k-ε-γ Equation Turbulence Model," *Journal of Fluid Mechanics*, Vol. 237, 1992, pp. 301–322.

[4] Raithby, G. D., and Torrance, K. E., "Upstream-Weighted Differencing Schemes and Their Application to Elliptic Problems Involving Fluid Flow," *Computational Fluids*, Vol. 2, No. 4, 1974, pp. 191–206.

[5] Chien, K. Y., "Predictions of Channel and Boundary-Layer Flows with a Low-Reynolds-Number Turbulent Model," *AIAA Journal*, Vol. 20, No. 1, 1982, pp. 33–38.

[6] Barbin, A. J., and Jones, J. B., "Turbulent Flow in the Inlet Region of a Smooth Pipe," *Journal of Basic Engineering*, Vol. 85, No. 1, 1963, pp. 29–34.

[7] Richman, J. W., and Azad, R. S., "Developing Turbulent Flow in Smooth Pipes," *Applied Science Research*, Vol. 28, No. 6, 1973, pp. 419–441.

[8]Martinuzzi, R., and Pollard, A., "Comparative Study of Turbulence Models in Predicting Turbulent Pipe Flow Part I: Algebraic Stress and k-ε Models," *AIAA Journal*, Vol. 27, No. 1, 1989, pp. 29–36.

C. G. Speziale
Associate Editor

Sound Amplification by a Supersonic Jet

V. G. Pimshtein*
Central Aerohydrodynamic Institute, 107005, Moscow, Russia

Introduction

THE possibility of amplifying sound waves incident on a shear layer is indicated in Ref. 1. This numerical–analytical work shows that, at certain angles of incidence, for the sound wave on an infinite linearly stabilized shear layer with a relative Mach number $M > 2\sqrt{2}$, the amplitude of the reflected waves is much greater than the incident wave amplitude. It is noted in Ref. 2 that in the case of sound excitation of a supersonic jet shear layer (at $M < 2\sqrt{2}$) the intensity of sound waves radiated by such a jet at the external excitation frequency can also exceed the intensity of the incident sound wave. Despite an apparent similarity of these phenomena, the essential distinction is that in the first case a reflected wave is considered. Its reflection angle depends on the sound incidence angle to the shear layer. In the second case, the sound radiation by a supersonic jet at the external excitation frequency occurs in a direction independent of the sound incidence angle. This relates to the radiation of Mach waves by disturbances arising in the shear layer under the action of sound and moving with a supersonic convective velocity along the jet boundary.[3] In this work it is also shown that the amplitude of disturbances arising in the supersonic jet at the nozzle exit depends on the sound incidence angle to the jet boundary. The most intensive disturbances arise in the jet for oblique sound incidence to the jet boundary. It is possible to expect that the intensity of sound waves radiated by the supersonic jet at the external excitation frequency also depends on the sound incidence angle to the jet boundary. In the present work the possibility of sound amplification of a sawtooth-like sound wave incident on the supersonic jet boundary is considered.

Results and Discussion

The investigations were carried out in an anechoic chamber of the Acoustic Division of the Central Aerohydrodynamic Institute with an isothermal supersonic air jet issuing from a conical supersonic nozzle designed for $M = 2.0$ with an exit diameter $d = 20$ mm. The total pressure P_0 in the settling chamber of the nozzle varied from 3.9 to 15.6 atm. A Hartman generator (HG) was used as the sound source ($f = 10$ kHz; Fig. 1). Its central core moved along an arc of 100-mm radius, with its center on the nozzle lip nearest to the sound generator. The angle β between the jet flow direction and the direction to the sound source varied from 90 to 140 deg.

Acoustic measurements (rms value of the sound pressure) were carried out with a Bruel and Kjaer microphone, Model 4136, moving along an arc of 40-mm radius with its center on the nearest nozzle lip, as shown in Fig. 1. The angle between the jet flow direction and the direction on the microphone varied from 20 to 35 deg. Analysis of the data obtained was made with a Bruel and Kjaer spectrometer, Model 2034, where the accuracy of the data obtained is ± 1 dB. The location of the measurement point was chosen to approach the radiation source in the jet as closely as possible and, on the other hand, to keep the microphone out of the hydrodynamic near field of the supersonic jet. To remove the influence of high pressure fluctuation levels generated in the near field of supersonic jets, all of the measurements were performed at the fundamental frequency of the HG. In the experiments, the sound pressure level (SPL) on the nozzle lip at the fundamental frequency was 146–148 dB. The SPL produced by the undisturbed jet and the HG at the measurement points at the fundamental generator frequency varied from 125 to 135 dB, according to the jet issuing regime and the measurement point position. Visualization of flow and sound waves was carried out with a direct shadowgraph technique using a spark source. (The size of the luminous body was 0.8 mm, and the exposure time was 2×10^{-7} s.)

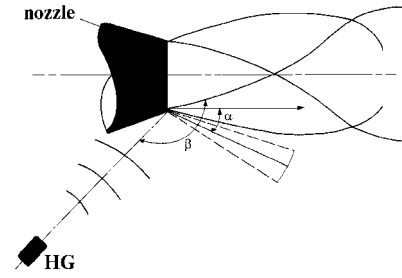

Fig. 1 Scheme of the experiments.

A typical shadowgraph, indicating the main features of the phenomenon under consideration, is presented in Fig. 2, which shows an incident sawtooth-like sound wave, disturbances in the jet formed under acoustic excitation, and Mach waves. (The incident sound wave propagation direction and the Mach waves radiation direction are indicated by arrows.)

The directionality of the radiated sound on an arc of 40-mm radius ($\beta = 130$ deg) shows that, under the action of sawtooth-like sound waves of sufficiently high intensity, the sound amplification does occur (Fig. 3). The intensity of sound radiated by the jet at the fundamental frequency (for HG and jet parameter values under investigation) can exceed the intensity of sound in the incident wave at the nozzle lip by up to 20 dB. At subcritical values of the jet total pressure, the convective velocity of the disturbances is less than the sound speed, Mach wave radiation is absent, and the sound intensity at the measurement points corresponds to the SPL in the incident wave (curve 5 in Fig. 3).

The most significant sound amplification is observed at oblique sound incidence to the jet boundary at the highest values of the jet total pressure investigated. If the sound incidence angle to the jet decreases, the intensity of sound radiated by it, as a rule, decreases. Thus, the influence of the jet total pressure on the intensity of sound radiated by the jet also decreases, but the tendency remains that under other constant conditions the jet with the higher total pressure value radiates the sound of higher intensity.

It seems evident that the possibility of sound amplification of a sawtooth-like sound wave incidence on the supersonic jet boundary is associated with the appearance and propagation of reasonably intensive disturbances, along the jet boundary, that are accompanied by Mach wave radiation. As the tests conducted have shown, the greater their intensity at the constant sound wave angle of incidence to the jet, the more the SPL is in the incident wave. Increasing the Mach wave intensity at sliding angles of incidence to the jet, in comparison with the case of normal sound incidence at constant values of SPL on the nozzle lip, is evidently connected with an increase in the amplitude of the disturbances. As a possible reason for this increase in the disturbance amplitude, it was suggested that there was a possibility of sound wave energy transfer to the vortex motion when the disturbances displaced the jet boundary.[3] However, it was noted that such treatment was not the only one possible. Another possibility is that the interaction of a sawtooth-like sound wave of a finite amplitude with a supersonic jet occurs in an extremely small time and space interval. It occurs when the zone of the maximum sound wave compression phase passes through the nozzle exit and is localized close to the nozzle edge. In this case, the sound incidence angle influence can consist of producing certain favorable ratios between the velocity of spreading the maximum compression phase in the incident sound wave over the nozzle edge and the phase speed of the vortex separation location shift from the nozzle lip. Evidently,

Received July 19, 1997; revision received Sept. 1, 1998; accepted for publication Sept. 30, 1998.

*Senior Research Scientist, Acoustic Division, TsAGI, 17 Radio Street.